Progressive collapse analysis of Hongqi Viaduct: a multi-span simply-supported bridge

Kaiming Bi[1], Hong Hao[2]

1. Corresponding Author. Lecturer, School of Civil and Resource Engineering, The University of Western Australia, WA.
   Email: kaiming.bi@uwa.edu.au

2. Professor, School of Civil and Resource Engineering, The University of Western Australia, WA.
   Email: hong.hao@uwa.edu.au

Abstract

Hongqi Viaduct, a multi-span simply-supported bridge in Zhuzhou, China, collapsed progressively during the mechanical demolishing of the bridge on May 17, 2009. The accident resulted in the loss of 9 lives and 16 injuries. This paper numerically simulates the collapse process of the bridge by using explicit finite element code LS-DYNA. The domino-type progressive collapse of the bridge is clearly captured, and the reason for the failure is discussed.

Key Words: Hongqi Viaduct, domino-type progressive collapse, numerical simulation, failure analysis

1. Introduction

The spread of an initial local failure from element to element, eventually resulting in the collapse of an entire structure or a disproportionately large part of it has been known as “progressive collapse” [1]. Progressive collapse takes place when the loading pattern or boundary conditions of the structure changes such that structural elements are loaded beyond their ultimate capacity and fail. When any element fails, the remaining elements of the structure seek alternative load paths to redistribute the load applied to it. As a result, other elements may fail as well [2]. Progressive collapse is characterized by a distinct disproportion between the triggering event and the resulting widespread collapse [3]. These initial triggering events may include, for example, gas explosion, blast, foundation failure, vehicle or ship/barge impact, fire, earthquake and wind loads.

Many bridge progressive collapse incidents have been reported in the history. These incidents include for example, the collapse of the Tacoma Narrows Bridge [4], the Silver Bridge [5], the Haeng-Ju Grand Bridge [3], the Tuojiang Bridge [5], the I-35W Mississippi River Bridge [6] and more recently the Hongqi Viaduct, the subject of this paper.

Numerical simulations of bridge progressive collapse are limited. This is because progressive collapse is a nonlinear dynamic process, which makes the quantitative analyses of progressive collapse quite complicated. Moreover, a detailed numerical model is usually required to realistically capture the collapse process of the structure, which makes the problem very time consuming and more daunting. This paper presents a case study on a typical multi-span simply-supported bridge, which collapsed progressively during the mechanical demolishing of the bridge. A detailed 3D finite element model, including the bridge slabs, wall-type piers, longitudinal and transverse reinforcement bars, is developed based on ANSYS [7]. The non-linear material behaviour including the strain rate effects of the concrete and steel rebar are considered. The nonlinear dynamic analyses are carried out by using the explicit finite element code LS-DYNA [8]. The domino-type progressive collapse process is replicated and the reason for failure is examined.

2. Honqi Viaduct

2.1. Bridge overview

Hongqi Viaduct is a multi-span simply-supported bridge located in Zhuzhou, China. It includes 121 piers and 122 spans, with 15 spans of length 13 m, 3 spans of 18 m and 104 spans of 20 m. The total length of the bridge reaches 2329 m. Fig. 1 shows the bridge before collapse. Each span consists of 16 prestressed concrete hollow slabs. The height of each slab is 0.85 m and the width is 1 m. The total width of the superstructure is 16.5 m with an equivalent density of 2241 kg/m^3. The height of the wall-type pier is 7.875 m from the pile cap and the thickness is 0.8 m. Fig. 2 shows the numbering of the slabs and the cross sections of the pier.

Fig.1. Typical view of Hongqi Viaduct (before collapse).

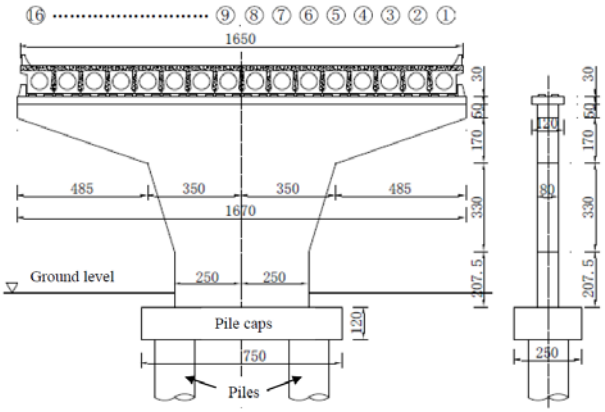

Fig. 2. Numbering of the slabs and cross sections of the pier (unit: cm)

Fig. 3 shows the reinforcement bars in the piers. Deformed steel bars with diameter of 1.8 cm (ϕ18) were pre-buried in the pile cap. The length of these pre-buried bars is 267.5 cm with 60 cm buried in the pile cap and the spacing is 8 cm. The size of the rest vertical bars is 1.2 cm (ϕ12), and the spacing varies with the height of the pier, with 8 cm between sections A-A and B-B, 16 cm between sections B-B and C-C and 24 cm between section C-C and the top of the pier. The transverse stirrups are round steel bars. The diameter is 1.0 cm (ϕ10), and the spacing between the transverse bars is 25 cm.

2.2. Demolishing scheme and progressive collapse

The original scheme of mechanical demolishing was to remove the connections between two hollow slabs first, and then a hydraulic breaker located on the adjacent span would be used to break the first hollow slab. The broken hollow slab would drop to the ground due to the gravity load. Then the hydraulic breaker would move to break the second slab. This process would be repeated until the total 16 slabs being demolished successively. The breaking location of the slab by the breaker is about 1.4 m to the left end of the slab. Unfortunately the actual demolishing process did not exactly follow the original plan. On May 17, 2009, when demolishing the slabs between piers #110 and #109, the last 4 slabs, i.e. slabs 13-16 in Fig. 2, were demolished together first, and then the hydraulic breaker was moved to break the remaining 12 slabs, which resulted in the 12 slabs dropping to the ground simultaneously. The left ends of these 12 slabs dropped to the ground but their right ends collided with pier #109, generating a huge impacting force on the pier. The huge impacting force from the collapsing slabs on the pier, which was not designed to resist such an impacting force, seriously damaged pier #109 and made it collapse toward pier #108. Consequently, the left ends of the slabs between piers #109 and #108 dropped to the ground due to the loss of support (pier #109), and the right ends collide with pier #108, which in turn resulted in the collapse of pier #108. The following spans followed the same pattern and formed the domino-type progressive collapse as illustrated in Figure 6 below. However, the collapse did not progress to the whole remaining bridge spans but stopped at pier #101, which deformed toward pier #100 with an

angle of 30 degrees due to impact by the collapsed span but did not collapse as shown in Figure 4(d). The collapsed spans and piers are designed and constructed the same, the reason why pier #101 did not completely collapse as piers #109 to #102 is not exactly known. Because the post incident investigation concentrated on the collapsed spans, no further information is available on pier #101. In this study, only the collapse mechanism is investigated. Totally 8 piers and 9 spans collapsed in the incident, and the collapsed length reached 180 m. Fig. 4 shows the bridge after collapse. 9 people died and 16 were injured in the incident.

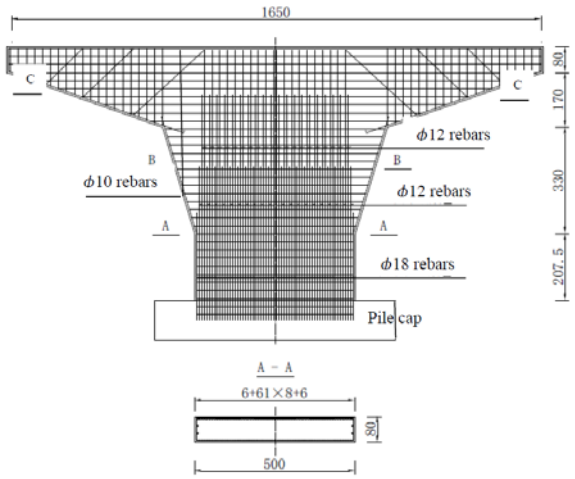

Fig. 3. Reinforcement bars in the pier (unit: cm).

Fig. 4. Hongqi Viaduct after collapse: (a) overview, (b) collapsed slabs, (c) remaining pier (#109) and (d) pier #101.

2.3. Site investigation

An investigation team was organized immediately after the incident. One important task of the team was to collect the concrete and reinforcement samples from the slabs and the piers. These samples were tested at the structural lab in Central South University in Changsha, China. The test results found that the average compressive strengths of concrete of the slab and pier are 64.1 MPa and 38.7 MPa, respectively. The average yield strength and ultimate strength of the reinforcement bars are shown in Table 1. These tested data are used in the numerical model of the bridge in this study.

Table 1. Average yield strength and ultimate strength of reinforcement bars

Size	ϕ18	ϕ12	ϕ10
Average yield strength (MPa)	347	498	470
Average ultimate strength (MPa)	526	571	574

3. Numerical model

A detailed 3D finite element (FE) model of the bridge is developed in the software package ANSYS, and the analyses are carried out by using the explicit finite element code LS-DYNA. Fig. 5 shows the elevation view of the FE model. To model the structural damage under impact loads and collapse, fine element mesh is needed, which usually results in huge FE models. To reduce the computational effort, without losing generality, only two spans and three piers (piers #110 to #108) are considered in the model. For the three piers, detailed modelling is only applied to pier #109, the pier that collapsed owing to the impact by the free falling span. In the detailed model the concrete and reinforcement bars are modelled separately, with constant stress solid elements for concrete and Belytschko beam elements for reinforcement bars. By conducting a numerical convergence test on

various mesh sizes (0.16, 0.08 and 0.04 m), it was found that the 0.08 m mesh yields similar results with the smaller mesh but with much less computational time. A mesh size of 0.08 m is therefore used to model pier #109 for both solid concrete elements and beam elements for reinforcement bars.

The penalty method is adopted to model the contact interfaces between meshes. The contact algorithm of *CONTACT AUTOMATIC SURFACE TO SURFACE in LS-DYNA is employed to avoid penetrations at the interfaces between bridge girders and the supporting piers. Slabs will drop to the ground after the demolishing part being removed, part ① will contact with ground, and part ② will collide with pier #109 and then slide to the ground along the surface of the pier. *CONTACT AUTOMATIC SURFACE TO SURFACE is adopted again to simulate these contacts. The contact type of *CONTACT AUTOMATIC NODES TO SURFACE is defined to model RC slab and reinforcement bar contact. Similarly, these two contact algorithms are defined to model the contacts between part ③ and pier #109. Since smeared model is adopted to simulate pier #108, only the *CONTACT AUTOMATIC SURFACE TO SURFACE is applied during the colliding and sliding process between part ④ and pier #108. The ground is modelled by keyword *RIGIDWALL, which provides a simple way of treating contact between a rigid surface (ground) and the nodal points of deformed bodies [8]. The bases of the piers are fixed in the simulation.

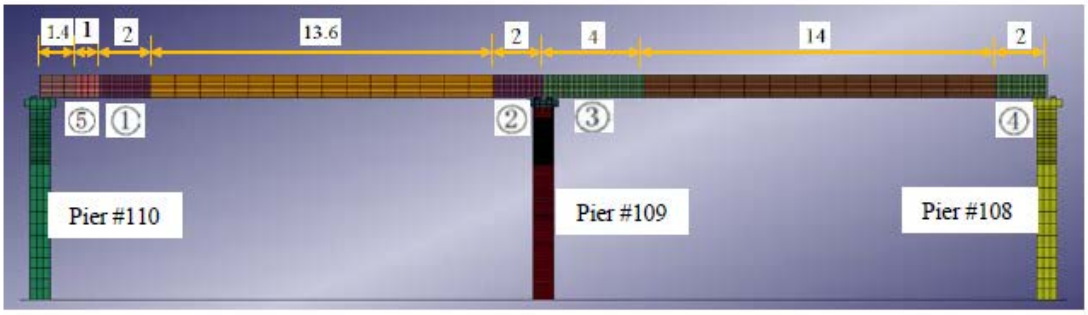

Fig. 5. Elevation view of the finite element model (unit: m)

Both *MAT CONCRETE DAMAGE REL3 (MAT_72REL3) AND *MAT ELASTIC (MAT_1) material models are utilised to model the concrete in the present study. MAT_REL3 model is employed at pier #109 where the damage of the pier will be modelled, while MAT_1 is used to model the smeared materials, i.e. piers #110 and #108 and slabs. In order to avoid computer overflow during calculation, the card *MAT ADD EROSION is used to eliminate elements that have been damaged and do not further contribute to load resistance. In the present study, the concrete in pier #109 will be deleted when the maximum principal strain reaches 0.3 or the tensile stress reaches 3.2 MPa. These two values are obtained based on a few trial-and-error tests.

The strengths of the structural materials are strain rate dependent as their dynamic properties can be enhanced significantly when subjected to high speed impact such as blast, barge impact or earthquake loading. Current study employs the dynamic increase factor (*DIF*), a ratio of the dynamic to static strength against strain rate to account for the material strength enhancement with strain rate effect. More detaield information about strain effect can be found from [9-11].

4. Numerical Results

4.1. Demolishing processes

As mentioned in Section 2.2, the last 4 slabs were demolished first followed by the rest 12 slabs simultaneously. The demolishing the last 4 slabs simultaneously did not cause bridge pier collapse but may generate some local damage to the pier. For simplicity, the damage induced by the impact from the falling slabs 13-16 is not considered. This will lead to some underestimation of the pier damage. However, the primary purpose of this simulation is to demonstrate that impact from 12

falling slabs is enough to collapse the bridge pier owing to the large impacting force and the pier is not designed to resist such a lateral impact. The results will show that even if the pier has no any prior damage, it is not strong enough to resist the impact.

In numerical simulations, since the explicit solver is used, the gravity load is applied. Applying gravity load induces the bridge structure to vibrate although it is applied slowly. This undesirable dynamic effect is removed by applying a large damping to the system [8] at the first 0.1 sec to make the system rest. After applying the gravity load the bridge is stable, Part ⑤ in Fig. 8 is then removed from the model.

Fig. 6 shows the collapse process of the bridge when the first 12 slabs are demolished together. Fig. 6(a) shows the model. Part ⑤ of slabs 1-12 is removed at 0.1 sec as shown in Fig. 6(b). The broken slabs drop to the ground due to the gravity load and impact the ground at 1.33 s as shown in Fig. 6(c). The left ends of the falling slabs move off from the bearing supports and impact on pier #109 at 1.44 s (Fig. 6(d)). Pier #109 begins to deform toward pier #108 after being impacted (Fig. 6(e)) by the falling slabs. Obvious shear failure occurs at about 2 m above the ground at Section A-A (Fig. 6(f)), where the cross sectional area changes as shown in Fig. 3. The reason of failure will be further discussed in Section 4.2. As also can be seen from the figure, the shear failure induced the collapse of pier #109. The upper part of the pier falls to the ground due to gravity, which results in the fall of the second span owing to the loss of support. The fallen upper part of pier #109 reaches the ground at 2.38 s (Fig. 6(g)), and it is eroded to avoid computer overflow due to large deformation and continuous contact. The second span drops to the ground at 2.92 s (Fig. 6(h)) and its right end begins to impact pier #108 at 3.13s (Fig. 6(i)). Pier #108 will collapse as pier #109 due to the impact loading, which induces progressive collapse of the bridge. However, in this study, to save the computational effort, damage of pier #108 is not modelled. As will be demonstrated in Section 4.2, the impact between the second span and pier #108 will lead to the collapse of pier #108.

The lower part of pier #109 below the shear failure section remains on the ground as shown in Fig. 7. The height of the remaining part is about 1.56 m in the numerical study, which is almost the same as that in Fig. 4(c), where the remaining part is about 1.63 m. This result also demonstrates that the model developed in the present study gives good predictions of the bridge failure.

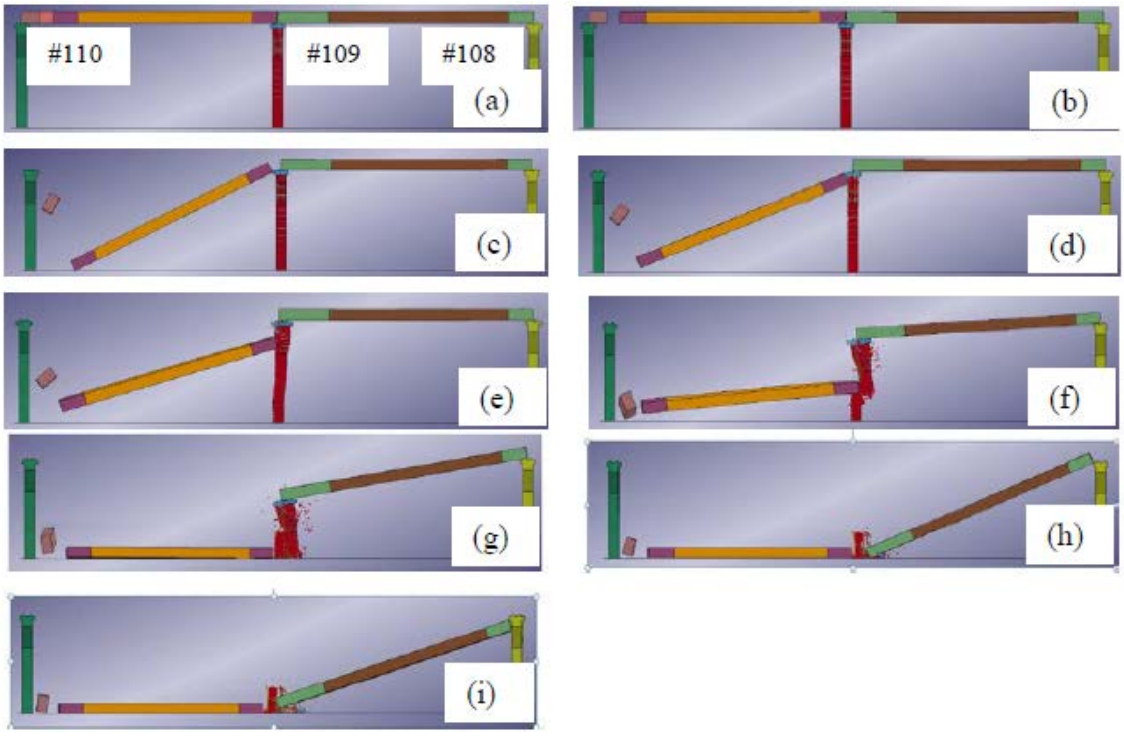

Fig. 6. Collapse process of simultaneously demolishing slabs 1-12: (a) t=0.0 s, (b) t=0.1s, (c) t= 1.33 s, (d) t=1.44 s, (e) t=1.60 s, (f) t=2.00 s, (g) t=2.38 s, (h) t=2.92 s and (i) t=3.13 s.

4.2. Failure analysis

As shown in Fig. 6, pier #109 is sheared off at section A-A because the shear force exceeds the shear strength of the pier. This section presents a simple analytical approach to assess this damage.

The nominal shear strength of the pier can be computed based on different design codes. For example, the ACI Building Code [12] and AASHTO specifications [13] take into consideration the concrete contribution (V_c) and steel contribution (V_s), and the nominal shear strength V_n is given as follows:

$$V_n = V_c + V_s \tag{1}$$

where

$$V_c = 2\left(1 + \frac{P}{2000A_g}\right)\sqrt{f_c'}b_w d \quad \text{(lbs)} \tag{2}$$

$$V_s = \frac{A_v f_{yh} d}{s} \tag{3}$$

In the above equations, P is the axial load (in lbs), A_g is the gross cross-section area (in in^2), f_c' is the concrete compressive strength (in psi), b_w is the width of the cross section (in in), and d is the distance from the extreme compression fibre to centroid of the tension reinforcement (in in), and $b_w d$ can be taken as $0.8A_g$. A_v is the area of transverse steel, f_{yh} is the yield strength of the transverse steel, and s is the vertical distance between hoops. With the parameters given in the previous sections, for section A-A shown in Fig. 3, it has $V_c = 4407.9\ kN$ and $V_s = 212.65\ kN$, and the nominal shear strength is 4620.55 *kN*.

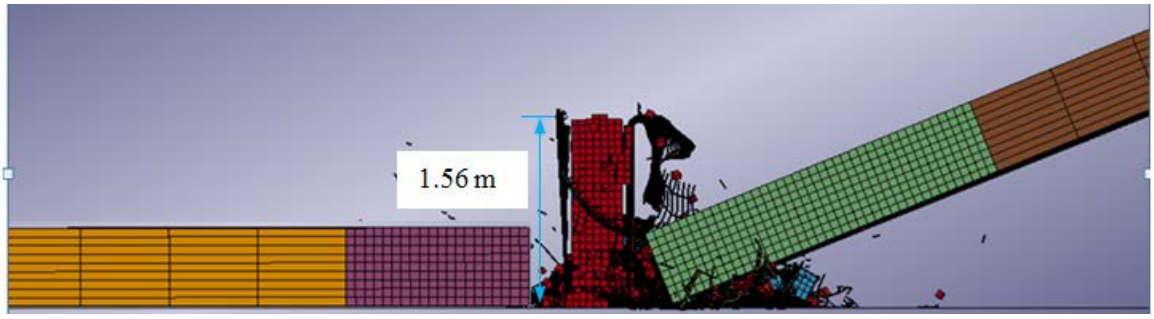

Fig. 7. The remaing part of pier #109.

When 12 slabs are demolished simultaneously, the maximum impacting force on pier #109 reaches 15.70 MN and the duration of the impact t_d is 0.05 sec as shown in Fig. 8(a). The first vibration period of the pier is T_n=0.176 sec based on a modal analysis. The impact force can be regarded as a triangular pulse as shown in the figure. For a triangular pulse, the dynamic amplification factor is about 0.9 when t_d/T_n =0.284 [14]. The de-amplified impacting force on pier #109 is thus 15.70× 0.9=14.13 MN, which is substantially higher than the nominal shear strength of the pie, therefore the pier collapses owing to insufficient shear strength to resist such a large impacting force. The horizontal impacting force on pier #108 from the impact of the falling span is 10.12 MN and the period is also 0.05 sec (Fig. 8(b)). The de-amplified impacting force is 9.11 MN, which is also larger than the shear strength of the pier, therefore pier #108 will collapse owing to insufficient shear strength like pier #109. Similar damage is expected to adjacent bridge spans and piers, leading to progressive collapse of the bridge structure. It is interesting to note that the impacting force on pier #108 is smaller than that on pier #109 although the weight of the falling superstructure is larger (16 slabs fall in the second span) than that of the first span (only 12 slabs). This is because of the partial support provided by the damaged pier #109 as well as the relatively longer span length which results in a slightly smaller impact angle.

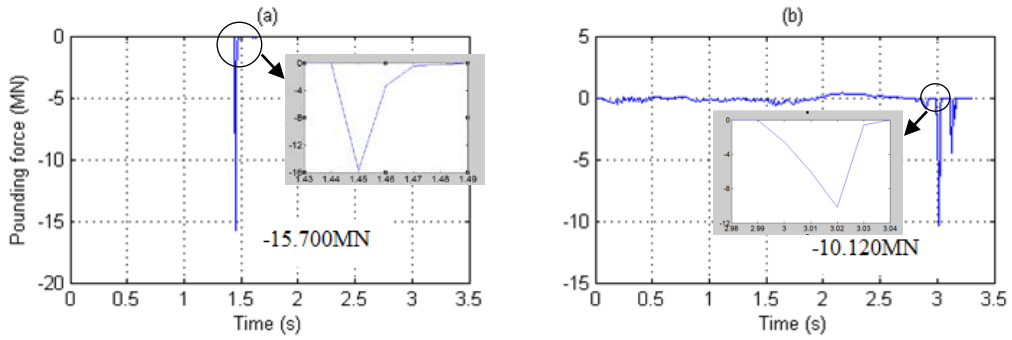

Fig. 8. Horizontal impacting forces on piers due to demolishing slabs 1-12: (a) on pier #109 from falling slabs 1-12, and (b) on pier #108 from falling 2nd span.

5. Conclusions

Hongqi Viaduct collapsed progressively during the mechanical demolishing of the bridge on May 17, 2009. The accident resulted in the loss of 9 lives and 16 injuries. This paper carries out numerical simulation on the bridge progressive collapse process. A simple analytical approach is presented to analyse the collapse. Following conclusions are obtained:

1. A detailed 3D finite element is developed to simulate the progressive collapse of the multi-span simply-supported bridge. The developed model captures the collapse process of the bridge.
2. The multi-support simply-support bridge supported by wall-type piers might be vulnerable to domino-type progressive collapse due to the limited shear strength of the supporting piers.

References:

[1] ASCE/SEI 7-05. Minimum design loads for buildings and other structures. NY: American Society of Civil Engineers; 2005.

[2] Salem SH, El-Fouly AK, Tagel-Din HS. Toward an economic design of reinforced concrete structures against progressive collapse. Eng Struct 2011; 33(12): 3341-50.

[3] Starossek U. Progressive collapse of structures. London: Thomas Telford; 2009.

[4] Lichtenstein AG. The silver bridge collapse recounted. J Perform Constr Fac 1993; 7(4): 249-61.

[5] Xu Z, Lu X, Guan H, Ren A. Progressive-collapse simulation and critical region identification of a stone arch bridge. J Perform Constr Fac 2013; 27(1): 43-52.

[6] Astaneh-Asl A. Progressive collapse of steel truss bridges, the case of I-35W collapse. In: Proceedings of 7th international conference on steel bridges, Guimaraes, Portugal; 2008. p.1-10.

[7] ANSYS. ANSYS user manual. ANSYS, Inc; 2002.

[8] LS-DYNA. LS-DYNA user manual. Livermore Software Technology Corporation; 2007.

[9] Comite Euro-International du Beton. Concrete structures under impact and impulsive loading. CEB Bulletin 187. Switzerland: Federal Institute of Technology Lausanne; 1990.

[10] Malvar LJ, Ross CA. Review of strain rate effects for concrete in tension. Amer Concr Inst Mater J 1998; 95(6): 735-39.

[11] Malvar LJ. Review of static and dynamic properties of steel reinforcing bars. Concr Inst Mater J 1998; 95(6): 609-16.

[12] ACI. Building code requirements for structural concrete (ACI 318-05) and commentary (ACI 318R-05). Farmington Hills, MI: American Concrete Institute, 2005.

[13] AASHTO. Standard specifications for highway bridges. 16th ed. Washington DC: American Association of State Highway and Transportation Officials, 1997.

[14] Chopra. Dynamics of structures: theory and applications to earthquake engineering. NJ: Prentice-Hall, 1995.